MRI Coil Development Strategies for Hybrid MR-PET Systems: A Review

Authors: Chang-Hoon Choi, Jörg Felder, *Member, IEEE*, Christoph Lerche, *Member, IEEE*, N. Jon Shah

This work was supported in part by the Helmholtz Validation Fund, "Next generation BrainPET scanner for 7 T MRI" Grant Nr. HVF-0051. C.-H. Choi (c.choi@fz-juelich.de), C. Lerche (c.lerche@fz-juelich.de) are with the Institute of Neuroscience and Medicine – 4 (INM-4), Forschungszentrum Jülich, Jülich, Germany. J. Felder (j.felder@fz-juelich.de) is with INM-4, Forschungszentrum Jülich, Jülich, Germany, with RWTH University, Aachen, Germany. N. J. Shah (n.j.shah@fz-juelich.de) is with INM-4 and INM-11, Forschungszentrum Jülich, Jülich, Germany, with JARA - BRAIN - Translational Medicine, Aachen, Germany and with the Department of Neurology, RWTH Aachen University, Aachen, Germany. Corresponding author: Chang-Hoon Choi (c.choi@fz-juelich.de).
Funded by the Deutsche Forschungsgemeinschaft (DFG, German Research Foundation) – 491111487.

Index Terms- **Antenna; coil; MRI; multimodal imaging; PET/MRI; PET-MRI; MR-PET**

Abstract

Simultaneously operating MR-PET systems have the potential to provide synergetic multi-parametric information, and, as such, interest surrounding their use and development is increasing. However, despite the potential advantages offered by fully combined MR-PET systems, implementing this hybrid integration is technically laborious, and any factors degrading the quality of either modality must be circumvented to ensure optimal performance. In order to attain the best possible quality from both systems, most full MR-PET integrations tend to place the shielded PET system inside the MRI system, close to the target volume of the subject. The radiofrequency (RF) coil used in MRI systems is a key factor in determining the quality of the MR images, and, in simultaneous acquisition, it is generally positioned inside the PET system and PET imaging region, potentially resulting in attenuation and artefacts in the PET images. Therefore, when designing hybrid MR-PET systems, it is imperative that consideration be given to the RF coils inside the PET system. In this review, we present current state-of-the-art RF coil designs used for hybrid MR-PET experiments and discuss various design strategies for constructing PET transparent RF coils.

1. Introduction

DRIVEN by recent technological advances, interest in the use of multi-parametric and multi-modal medical imaging techniques is expanding rapidly [1-6], and it is widely anticipated that the increased access to dynamic information afforded by these techniques will improve diagnostic accuracy and inform clinical decision-making in the future. Currently, magnetic resonance imaging (MRI) and positron emission tomography (PET) are two very commonly used diagnostic imaging technologies in standard clinical practice and preclinical research, with both modalities offering unique insights. MRI enables the imaging of high-quality morphological structures *in vivo* in conjunction with a lavish number of superb soft-tissue contrast mechanisms, while PET utilises a variety of radioactive tracers to target different metabolic and molecular pathways, providing highly specific and sensitive information relating to physiological and metabolic processes. The benefits of combining these features are clear, and the development of simultaneously operating MR-PET scanners have heralded the possibility of obtaining unique images with advantages afforded by each individual modality in a single exam [3-9]. However, despite the apparent advantages of combined MR-PET systems, technical challenges must be considered.

Several approaches to integrating MR and PET have been explored, such as the use of split magnets and light guides to place the detectors (photomultiplier tubes) outside the magnet [10, 11]. With the advent of magnetic field insensitive detectors, such as APDs and SiPM, these have been superseded by designs whereby a PET insert is placed inside the bore of the magnet. This approach combines MR and PET into a fully integrated system, enabling simultaneous acquisition of both MR and PET datasets [12, 13]. In such integrated systems difference can arise from the placement of the PET detectors which can be wholly inside the gradient coil or integrated into a split gradient coil [14].

For the MRI system to work, a radiofrequency (RF) coil or antenna is required for transmitting and/or receiving RF signals. For the RF coil to function effectively in MR measurements, it must be positioned close to the subject under examination, which is, in hybrid MR-PET systems, normally inside the PET active imaging region. This makes the combination of both modalities difficult since each modality has different specifications and requirements. For example, standard RF coils and antennas do not have the same requirements that are fundamental for PET, i.e. the use of low-density or no materials in the PET field-of-view (FOV), and are generally only designed for use in MRI, e.g. the use of non-magnetic materials. Thus, in hybrid MR-PET systems, the RF coils are very likely to contain materials that strongly contribute to attenuation and the scattering of gamma- radiation, such as capacitors, soldered joints or coaxial cables, and these are likely to be distributed at random locations in the PET imaging FOV. This results in count loss and the potential generation of artefacts [15-20]. Although it is possible to correct for the attenuation of the RF coil placed inside the FOV of PET, such corrections can be arduous, and artefacts may not be completely removed [19-21]. This results in significant quantification errors and degradation in the sensitivity of the PET images, a situation which is less than ideal. Therefore, to minimise any potential absorption and scatter of gamma-radiation, while at the same time

maintaining the maximum MR imaging capability without compromising image quality, e.g. high signal-to-noise ratio (SNR), it is crucial to take the bi-directional compatibility of materials into consideration when designing hybrid MR-PET systems.

This review presents an overview of the key strategical features of designing MRI coils for hybrid MR-PET systems. In this work, we mainly focus on brain applications, but the central principles can undoubtedly be employed to examine other areas of interest. The main body of this review includes a variety of design approaches and also considers the materials used for the construction of coil elements and coil formers. The coil design part is further divided into three subsections, and a detailed description of each strategy is provided, along with the associated novelties and importance.

II. CLASSICAL APPROACH: MOVING HIGH-DENSITY COMPONENTS AWAY FROM THE PET FOV

The most intuitive and simple way of designing a simultaneously operating MR-PET coil is to relocate the high- density compartments of conventional coils to outside the PET imaging region [22-28]. The high-density components of the coil mainly include various non-magnetic fixed capacitors and trimmers, inductors, co-axial cable bundles, etc. Since its first appearance in MRI in 1985, the birdcage coil has been one of the most ubiquitous transmit / receive MRI coils, offering the benefits of large volume coverage and a highly homogeneous RF field (B1) [29]. Depending on its configuration, it can normally be operated in a high-pass or low-pass mode. In the high-pass case, the required capacitors tend to be placed on the end-rings, whereas in the case of low-pass, the capacitors are positioned on each rung, which could be in the middle of the imaging FOV. Figures 1a and 1c exemplify the conventional, high- and low-pass birdcage coils, indicating where the potential high-density materials are located within the MR- PET imaging FOV (highlighted using light red shading). Figures 1b and 1d show how to reposition the capacitors to avoid them being inside the PET detection field-of-view – namely by extending the overall length in the high-pass case (b) or by splitting the single capacitor into two arranged in series with one capacitor located on each end of the low-pass birdcage rung. Figure 1e is a photograph of the birdcage coil.

In the design introduced by Oehmigen et al., an existing commercial birdcage coil was modified in the same manner to fit the hybrid operation [28].

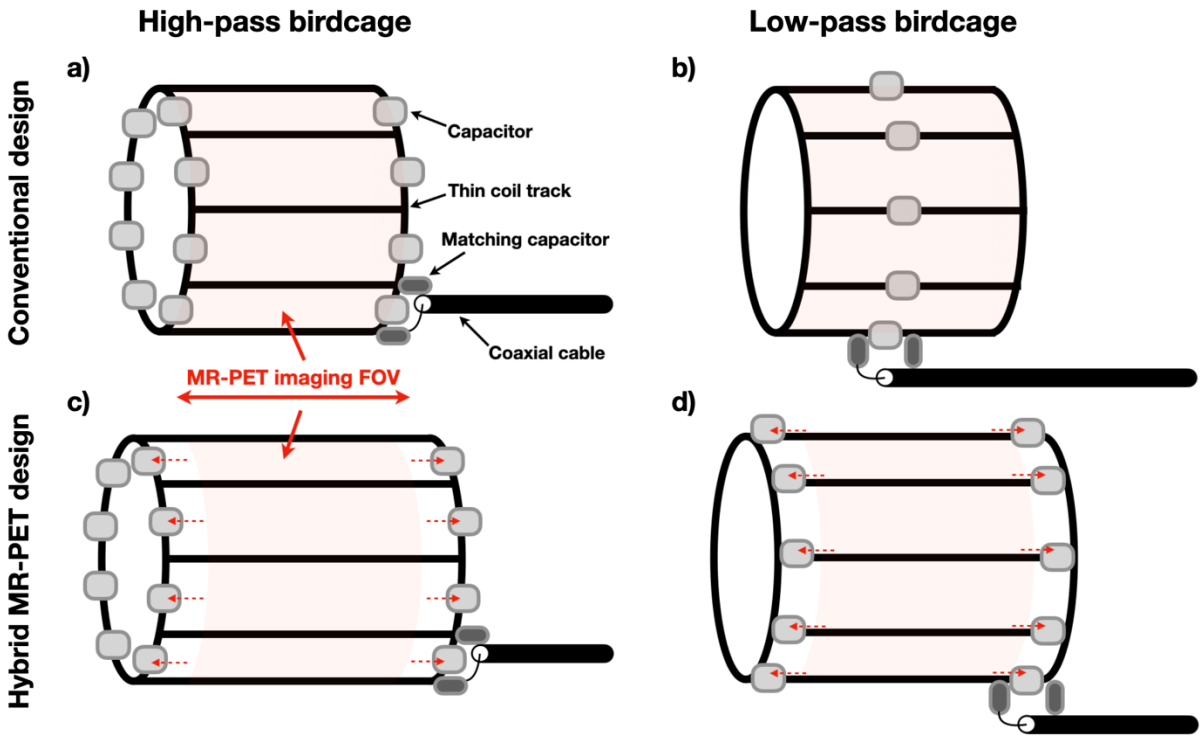

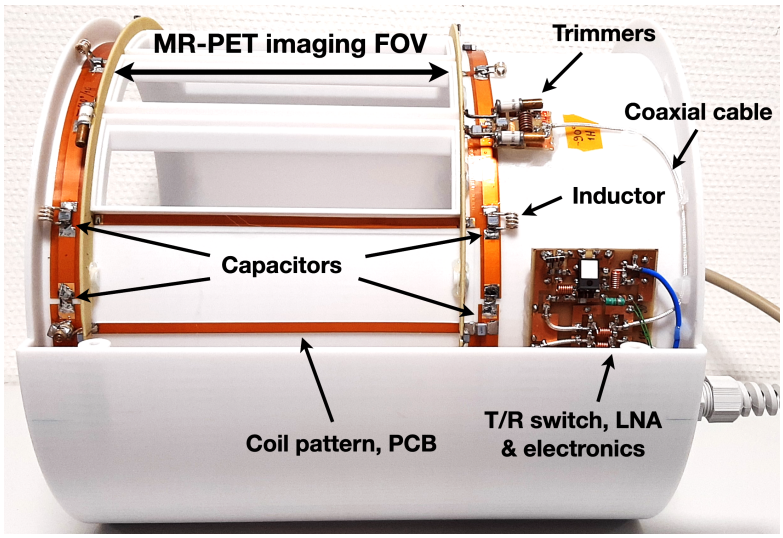

Figure 1. Conventional high-pass (a) and low-pass (b) birdcage coils showing the location of the high-density materials, and modified high-pass (c) and low-pass (d) birdcage coils for simultaneous MR-PET. A photograph (bottom) of the double-tuned birdcage coil recaptured from the reference [20]. This comprises two birdcages: low-pass flat design for ^{31}P nucleus detection and high-pass folded design for ^{1}H.

Since then, this approach has been applied to various coil designs, not only for birdcage coils [21, 26, 28], but also for surface coils [23], and even for multi-channel arrays [24] and double-tuned coils [26-28].

Although the goal of building a PET-compatible MRI coil can clearly be achieved using this design, it may not be the optimal choice as the quality of MR images are unlikely to be as good as that of the stand-alone, standard coil frequently used in MRI. This drawback mainly comes from the extended length of the coil, which leads to a reduction in SNR and a restriction in the dimension (e.g. shoulders for the brain/head imaging applications). The current clinical default setting at 1.5 and 3 T is to combine a large body transmit coil, together with a number of small multi-channel receive-only coils, which provide the uniform B1 transmit-field as well as high sensitivity [30-32]. In addition to not using a multi-channel receive array, this volume coil design also prevents the possibility of using parallel imaging techniques, which require the use of multi-element coils to exploit sensitivity profiles of the individual elements, or fast acquisition techniques, which perhaps brings an additional restriction for certain applications requiring high SNR, high-resolution or a short scan time [33, 34].

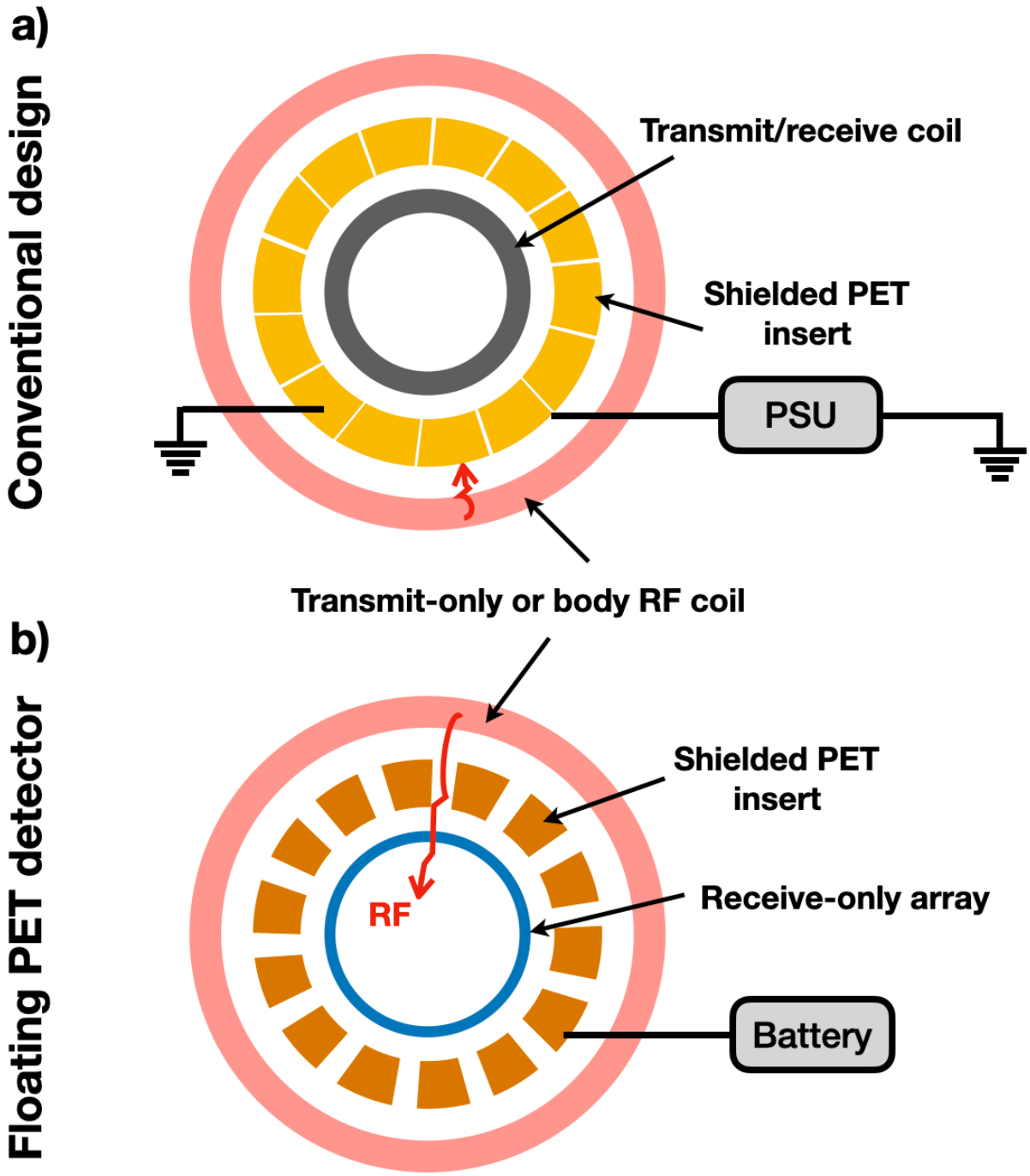

Figure 2. Designs of a conventional (top) and an RF penetrable, floating PET insert (bottom) redrawn from the reference [24].

III. RF PENETRABLE OR RF-COIL-INTEGRATED PET INSERT

The next approach to designing MR coils for integrated MR-PET systems is to use an RF-penetrable or an RF-coilintegrated PET insert. The main factors to consider with this approach are that it requires a modification of the PET detectors, thus making the PET modules unconventional, and due to the position of the coil, the integrated RF shield also needs to be altered. MRI scanners are mostly placed inside a Faraday cage to prevent any unwanted RF interference from the surroundings, and due to the inter-directional interference, the PET systems inserted inside the MRI scanner would need to be completely shielded [35-37]. In this manner, an interference-free, simultaneous MR-PET operation can, in principle, be achieved. MR coils working within the RF range are very sensitive to shields made of copper or aluminium, and basically, the shield blocks the penetration of the radiofrequency. Depending on the shield position or the distance between the shield and the coil, the performance of the coil, particularly its efficiency and sensitivity, can be substantially influenced [38]. Due to this, the PET system is likely to be positioned outside the body coil in integrated MRPET systems that are commercially available for clinical use, thus mitigating deleterious effects on the MR system [39].

However, this may not be ideal with respect to the PET performance, and importantly, increased costs due to an increased diameter of the PET ring.

A. RF penetrable, floating PET insert design

As introduced previously, the use of a multi-channel receive-only array together with a body transmit coil in MRI is a well-established configuration at clinical field strengths, i.e. 1.5 and 3 T. Here, the body coil is always included, which is mostly used for transmitting RF or for imaging large volumes, while the receive array is only used for signal reception. However, in order to improve the quality of the PET system for brain applications and to make it easily adaptable to existing MR scanners, the PET system is often designed as an insertable unit, which is normally installed into the magnet bore [4-6, 16, 22, 24]. For simultaneous imaging, however, this shielded PET insert system prevents the use of the built-in body coil in the MRI scanner. Consequently, a great number of MR coils for simultaneous MR-PET measurements are designed as transmit/receive volume coil styles. The option of having separate transmit and receive operation is not possible due to the requirement of a multi-layer design, potentially leading to more attenuation and space restriction. In particular, transmitting requires more power, so the components and cables for transmit coils are mostly made of larger, thicker and more dense materials, leading to higher attenuation.

In order to cope with these challenges, a group from Stanford proposed and constructed an RF penetrable, floating PET insert that could be incorporated into a clinical MRI scanner [24, 40-42]. The most interesting point of this strategy was the option that enabled the standard MR body coil to be used for RF transmission. Figure 2 illustrates the proposed floating PET insert design (Fig. 2b) in comparison to the conventional model (Fig. 2a). Using various strategies, e.g. optical signal transmission and battery

power source and noise removal, they were able to make the PET insert both MR compatible and RF penetrable.

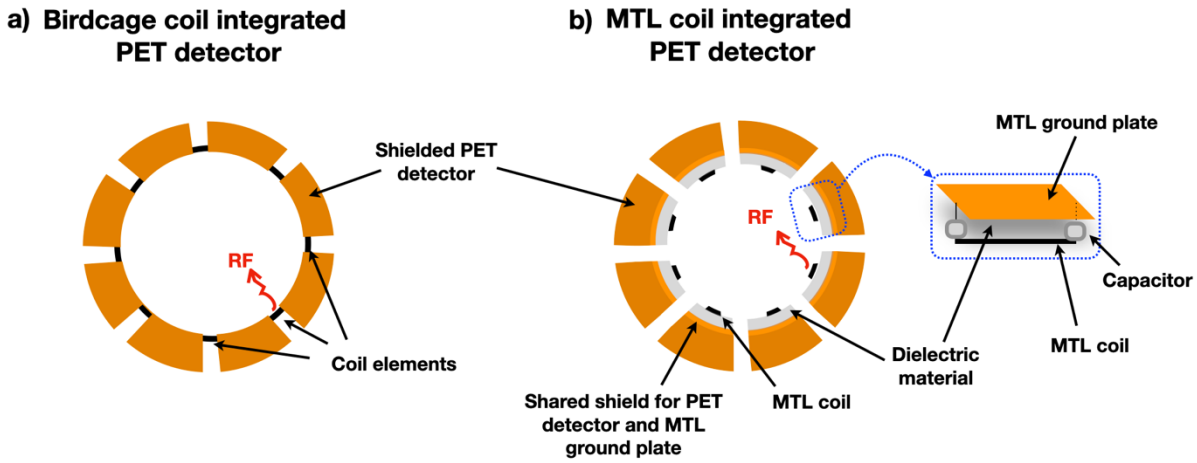

Fig. 3. An 8-rung birdcage coil (a) and an 8-channel MTL array (b) integrated into the shielded PET detector module. A single channel zoomed MTL coil is also shown. Images were recreated based on the references [43, 44].

In this approach, the B1 transmit-field was generated through tiny gaps between the PET detector modules and some degree of uniform B1 field (with about 30% degradation) was accomplished inside the PET FOV. However, even though the MR performance could be further improved by using a receive-only array, they reported a reduction in transmit efficiency of approximately 35% and artefacts (e.g. checkerboard pattern) on their MR images compared to those without the floating PET insert. Furthermore, it should be mentioned that the gaps between the PET detectors in the floating design will inevitably lead to a small loss of PET sensitivity compared with a conventional design.

B. RF-coil-integrated PET insert design

As mentioned above, the birdcage coil is one of the most commonly used MRI coils and attempts have been made to integrate an 8-rung, high-pass birdcage coil into a home-built PET insert [43]. In this approach from Akram et al., the birdcage rungs are positioned between two shielded PET detector modules. Figure 3a shows the conceptual drawing of the geometry of the birdcage elements from the viewpoint of the z-axis. The design was assessed by comparing a number of important MR factors, i.e. B1 homogeneity, SNR and local/global specific absorption rate (SAR). Due to the same effects associated with the closely placed shield described above, they found a degradation of approximately 5% in B1 uniformity, 60 to 70% in SNR and around 20% to 60% in SAR, which varied depending on the MR sequence of choice.

Even though the PET performance was not compared as a function of the size of the gap, it was anticipated that this modification could degrade the sensitivity of the PET since the segmented PET ring could reduce the amount of gamma quanta captured.

Another modification proposed by the same group was to use a microstrip transmission line (MTL) resonator [44]. MTL is also a popularly used MRI coil at higher field strengths (> 3T) and has a special feature that the coil is supported by a ground plate and dielectric material between the MTL and the

ground plate. The design strategy suggested by the authors was to share the ground plate for both the MTL resonator and the PET shield simultaneously. As shown in Fig. 3b, whether the ground shield is in the form of a plate or a box makes no difference in the coil characteristics in terms of MRI. Thus, this tactic could be greatly beneficial and also allows space to place the integrated PET insert within the RF coil. However, since the use of dielectric material is particularly recommended at higher field strengths, it is possible that the ground shield would attenuate the gamma-radiation.

Furthermore, this concept was only demonstrated using a 4- channel MTL array, where one would expect the coupling factor among the elements to be good enough. However, if the number of channels was to be increased to, e.g. 8-channel in order to improve the B1 homogeneity, the MTL array may require the additional employment of decoupling techniques to minimise the interference among each coil element [45]. Attaching the decoupling circuits may result in increased attenuation and degradation of the PET performance. Nevertheless, the PET detectors can be positioned close to the subject and, therefore, it may have a potential improvement in the PET sensitivity and resolution, which may compensate the loss stated above. In the case of Fig. 3a, attenuation correction of the embedded coil may also not be required as it stays outside the PET FOV which can be an additional advantage.

Overall, these design strategies may influence PET performance, and in most cases, could restrict system flexibility. On the other hand, integrating conventional MR coils into the PET insert could result in a compact and independent insert with a combined all-in-one design. The former, i.e. the RF-penetrable PET insert, has the great advantage of allowing the use of the existing integrated MR body coil for transmission at clinical field strengths. Due to the closely placed, shielded PET insert, however, the transmit efficiency could significantly decrease, requiring the application of much higher RF power. This, therefore, might preclude the running of short and high amplitude RF pulses and may increase SAR values at high fields [46].

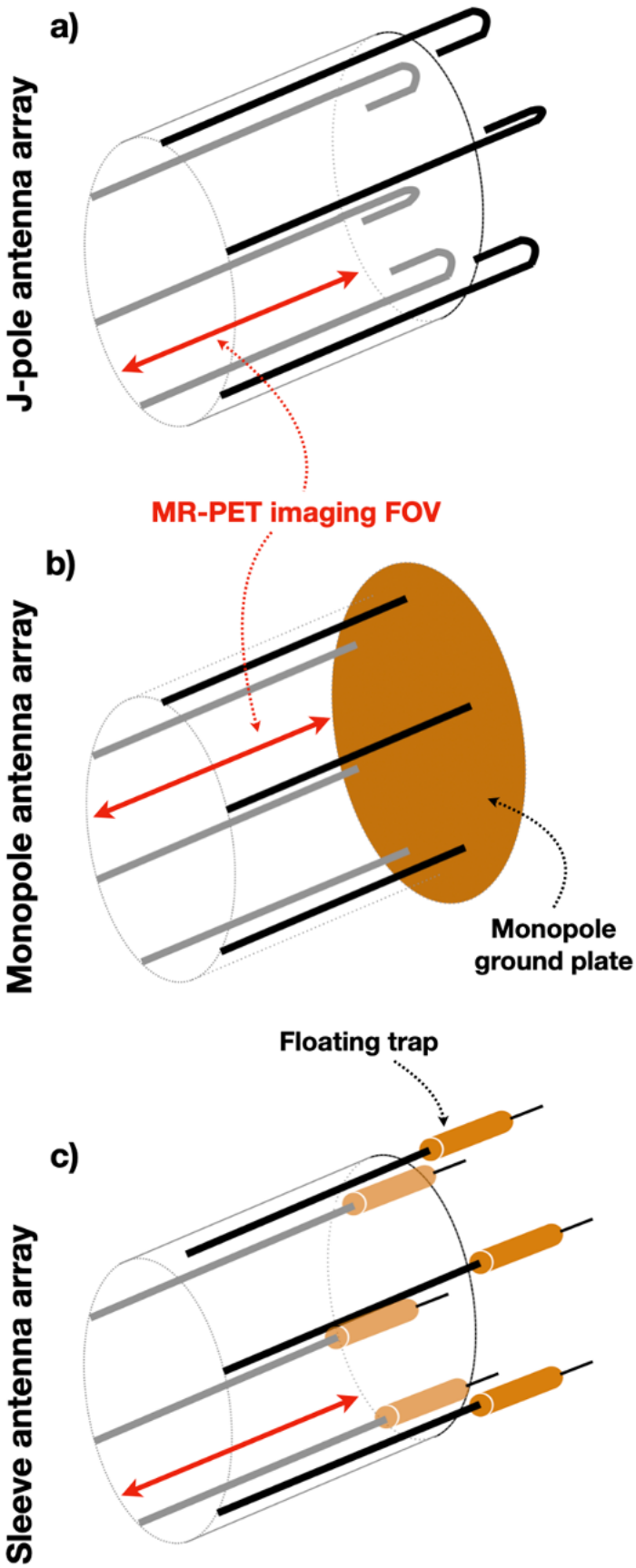
a)
J-pole antenna array
MR-PET imaging FOV
b)
Monopole antenna array
Monopole
ground plate
Floating trap
c)
Sleeve antenna array

Fig. 4. Schematic diagrams of novel MRI antenna arrays which have the potential to be used for simultaneous MR-PET acquisitions: a) J pole antenna, b) monopole antenna and c) sleeve antenna. Images were drawn on the basis of the references [57, 59, 66].

The RF penetration efficiency can be improved with different arrangements of the shielded PET insert i.e. by splitting one to two in the z-direction or by increasing the gaps between adjacent modules [47]. However, the large gaps between PET modules lead to the generation of mandala or chimney artefacts [48]. Thus, the gap size is a trade-off and requires further optimisation, which can increase the path rate of the RF but also degrade the PET performance.

IV. STRATEGIES USING EMERGING TECHNOLOGIES: NOVEL MR ANTENNA ARRAYS

As MR sensitivity increases proportionally to the main magnetic field strength, MRI systems operating at higher field strengths have the potential to offer higher resolution and higher SNR, possibly resulting in a shortening of the required scan time in comparison to lower field strengths [49]. Thus, there has been an increased tendency towards stronger field strengths, and the usefulness of ultra-high field (UHF) MRI systems has been demonstrated in various clinical applications [50-52]. In addition to MR technological developments, there have been several attempts to integrate PET systems into UHF MRI using new PET detector technologies [53-55]. Besides the previously discussed challenges associated with MR-PET integration, human imaging at UHF poses further challenges, mainly resulting from the non-uniform B1 fields that occur due to a shortened RF wavelength and higher SAR in tissues [47].

In order to compensate for these obstacles, various new methods and approaches have been introduced, including the use of radiating antennas together with parallel transmission techniques [56-62]. To date, mostly dipole antennas, used as radiating antenna, have been investigated and demonstrated in humans and have become a standard coil for use in UHF MRI [56, 63, 64]. Unfortunately, the dipole antenna array is not the best candidate for simultaneous MR-PET systems due to its centre feeding configuration (containing high-density materials, i.e. capacitors and coaxial cables), leading to high gamma-absorption and scattering [57]. Thus, having to take the fundamental necessities of PET into consideration, in addition to the standard requirements of UHF MRI, makes developing an RF antenna array even more complicated and difficult. However, despite not being frequently used in UHF MRI, several new antenna designs are emerging.

Figure 4 illustrates how these novel antennas are organised, along with the PET imaging region. These designs, by virtue of the fact that there is inherently little material in the PET FOV, are expected to be most suitable for hybrid MR-PET [57, 65, 66].

Choi et al. recently invented a J-pole antenna array (Fig. 4a) and demonstrated its potential use for simultaneous MR-PET and MR-SPECT [57, 67]. The MR performance of the J-pole antenna array was compared against the standard dipole antenna array, and the gamma-radiation transparency was presented [57]. The results showed that the MR performance was comparable to the reference, while the PET performance was significantly superior, as indicated in Fig. 5. It was possible to achieve PET transparency since the J-pole array only included antenna patterns made of very thin (few μm) copper strip, and none of the lumped components were accommodated inside the PET imaging FOV. Furthermore, as these antennas can be driven by one side of the antenna through cable traps attached to coaxial cables, it is possible to use them in hybrid imaging modalities.

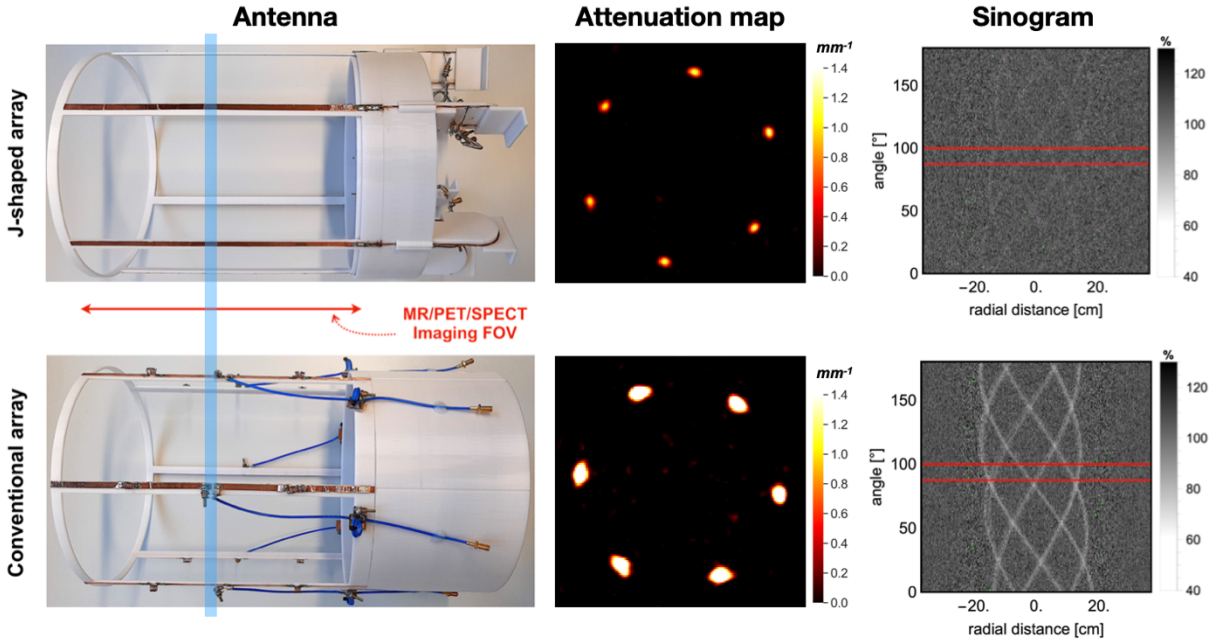

Fig. 5. A photograph of one of the emerging antenna arrays with the potential to be used as an MR-PET coil along with its attenuation map and sinogram. Top: J-pole antenna array and bottom: Dipole antenna array. The blue box indicates the slice for the attenuation maps and sinograms as measured according to the antenna arrays. The images were modified from the reference [57] with the copyright permission granted through RightsLink®.

Figure 5 shows comparison pictures and maps of gammaradiation-attenuation between the J-pole antenna array (top) and a dipole antenna array (bottom), which is an MRI coil commonly used at UHF. All of the components, as well as the feeding part, are relatively far away from the main imaging area, resulting in significantly reduced attenuation in the map. Although it has not yet been shown with PET, this strategy may, theoretically, be valid for other antenna designs, such as monopole antenna, shown in Fig. 4b [65] or a sleeve antenna, shown in Fig. 4c [66]. It can be seen from the figures that these antenna arrays also only require a simple and very thin conducting patterned line within the active imaging region. Here, the sleeve antenna is a modification of a monopole antenna, which combines with floating cable traps instead of using the ground plate. In this way, it could help prevent problems or artefacts in monopole antenna arrays, potentially caused by eddy currents.

V. CONSIDERATIONS OF BUILDING MATERIALS FOR COIL COMPONENTS AND FORMERS

In general, MRI coils consist of a range of different elements, including a coil itself which are made of nonmagnetic, conducting materials, mostly using copper or aluminium, coil cases for supporting and enclosing the coil, and, in some cases, an RF shield, also made using copper, aluminium or similar materials. The coil traces can be generated in the form of a printed circuit board (PCB), wire, pipe or thin tape. Due to its flexibility and precision, today coil cases are frequently manufactured with a 3D printer, using various plastic materials, e.g. biocompatible polycarbonate. As all these components are inside the sensitive PET imaging region, they all require careful consideration during the design stage.

Choi et al. designed several simple loop coils using various copper-based materials: pipe, strip, wires and flexible FR4 PCB and evaluated the characteristics of the coils at two different frequencies for 1H and 31P measurements by comparing quality factors for MRI and attenuation for PET [68]. They found that although copper pipe was the best conducting material for designing the coil for MRI, its gamma-radiation absorption level was rather significant (′ 6) compared to the other materials. Conversely, thin (~ 35 μm) copper strip and flexible FR4 provided very low gammaradiation attenuation with approximately 15% (to the pipe) lower quality factors. It has also been reported in the literature that such a thin conductor does not noticeably contribute to the attenuation [20, 26, 57]. Using transmission scans, Oehmigen et al. systematically studied the attenuation of a large quantity and range of individual materials commonly used to construct MRI coils, including homogeneous materials (e.g. different plastics, aluminium, copper and brass) and heterogeneous samples (e.g. ceramic capacitors, cables, inductors and soldering tins) [15].

The results acquired provided useful information for improving the quality of not only future MR-PET compatible coil development but also test phantoms and accessories, e.g. mirror systems for functional MRI or headsets for acoustic noise-reduction [69-71]. Additionally, Celik et al. took the coating material for the coil case into account, which should provide electrical insulation and be waterproof, but it may increment extra gamma-ray absorption [26].

Researchers also evaluated the feasibility of using multichannel receive arrays with PET [72-75]. Hope et al. designed a minimally attenuating 16-channel anterior body array and their attenuation level was comparable to the 4-channel torso array [72]. Anazodo and colleagues built a 32-channel head coil array using a coil array pattern based on aluminium rather than copper, since aluminium has theoretically lower absorption, and investigated its usefulness [74]. It was reported that the array constructed using aluminium did not appear in the attenuation map, making it ideal for use in simultaneous acquisitions. Moreover, the authors demonstrated the MR performance of the 32-channel aluminium coil array to be comparable to that of the 12- channel commercial copper coil array. Sander et al. obtained attenuation

maps of different conductors (i.e. aluminium foil, copper foil, 18 awg wire and 16 awg wire), coaxial cables (i.e. 1.2 mm and 2.2 mm diameter), preamplifiers and different sizes of plastic housing (i.e. 2 mm, 6 mm and 12 mm). Based on the MR image quality and PET attenuation, they suggested that smaller components are the optimum choice if they perform in a similar fashion to physically larger alternatives and recommended that all components be evaluated for their properties prior to building MR-PET coils [73]. Recently, Stickle et al. developed a foam-type coil former to replace a conventional rigid plastic former and found minimal PET interference. They also rearranged internal cables and tuning/matching/decoupling units in order to optimise the attenuation and the MR image quality [75].

VI. DISCUSSION AND OUTLOOK

Simultaneously operating hybrid clinical imaging systems are attracting increasing interest as they enable access to multiple biological parameters with good spatial and temporal resolution and have the potential to provide synergetic diagnostic information. Moreover, the simultaneous aspect is particularly useful for certain applications that require correlation and causality between neuroreceptor occupation and/or neurotransmitter release and brain activation, e.g. neuroimaging and neuroactivational studies. The fact that important physiological parameters, such as blood flow and blood volume, can be assumed to be the same – by virtue of simultaneous acquisition – during the acquisition of both image data sets is a critical advantage.

In this review, we have shown several previous efforts and possible design approaches relating to the construction of PET transparent MR coils that aim to maximise the image and performance quality of both modalities. In the context of MRI, using the transmit-only / receive-only configuration is rather challenging as it requires the location of essential components inside the PET FOV [73, 75]. In particular, the multi-channel loop arrays used for integrated MR-PET systems have to predominantly rely on attenuation correction since designing the array without the use of a number of soldered joints, capacitors and cables is unavoidable. Nevertheless, this combination is still recommended since it provides a uniform B1 field and higher detection capability and is suitable for use at higher field strengths, i.e. UHF, due to its increased sensitivity.

It is clear that using some emerging antenna designs, as introduced in the above section, is also an appropriate strategy for integrated MR-PET systems. These antenna arrays are capable of carrying out a transmit-only operation together with the use of parallel transmission techniques, or a transmit and receive function. Each antenna has its unique properties, which determines the physical size of the antennas. For example, the monopole or sleeve antenna has quarter-lambda, while the J-pole has half-lambda characteristics within the PET FOV. Thus, one could be more suitable than the other for particular applications, body parts or field strengths. To date, these antenna arrays have only been applied at field strengths higher than 7 T, and the optimal length of the antenna is suitable for these field

strengths. Nevertheless, a larger number of simultaneously operating MR-PET scanners are available at clinically relevant field strengths, such as 1.5 T and 3 T, and adaption to these lower field strengths would be advantageous as these antennas are almost PET-transparent.

Although we did not focus on the influence of RF shields, the primary reason for including a shield is to prevent the bidirectional interference between PET and MRI [35-37], which requires the complete shielding of the inserted PET system. Depending on its arrangement and materials, the shield attached to the PET detector can also play a pivotal role in antenna efficiency and homogeneity [35-37, 76]. Due to the space limitation associated with the use of a PET insert, in some cases, the shield on the PET module has to be placed close to the RF coil, and consequently, the efficiency of the RF coil is significantly affected, leading to considerable SNR loss. Conversely, at higher field strengths, the shield could benefit the performance of the coil array as it improves radiation loss, which is larger at higher frequencies [77].

However, the shield is often a potential source of eddy currents, which tend to disturb the gradient waveforms resulting in image distortion and artefacts. Thus, optimising the shield-to-coil distance and the eddy current characteristics on a hybrid system requires further investigation [35, 38, 78-

80].

An additional factor when considering the MRI coil is its role in providing anatomical information covering the entire PET FOV, enabling the generation of an attenuation map to aid accurate PET image reconstruction. Two of the most widely used methods for attenuation correction (AC) in the field are to derive the required attenuation maps using either computer tomography (CT), with an application of extrapolation to 511 keV, or transmission scans (TS), with an external radioactive source of ideally 511 keV [81, 82]. Both methods, however, have drawbacks that lead to systematic errors in the reconstructed attenuation corrected PET image [83]. The precision of the former approach is generally restricted by the requirement that it needs to convert a linear attenuation coefficient (μ-value) obtained from a continuous X-ray spectrum to a μ-value corresponding to the inherent monoenergetic spectrum of PET. For example, AC maps are normally generated using a clinical CT scanner (typical photon energy range: 30 keV ~ 140 keV), requiring an extrapolation to 511 keV. The widely used bilinear scheme to convert from Hounsfield units to μ-values for human tissue [84] is inappropriate for the highly attenuating coil components [83]. Conversely, extrapolation is not required in the latter method as it is based on measurements with rotating 511 keV sources. However, unfortunately, PET scanners with integrated rotating transmission sources are no longer produced, and the AC mapping of an RF coil is different to the one used for the combined MR-PET scan. This leads to systematic errors caused by mismatch of the spatial resolution of both PET systems involved [85] and also to the incorrect alignment of the AC map for PET image reconstruction, which is caused by the fact that the transmit/receive coil is generally

not visible in either the MR image or the PET image [83]. The location of rigid coils can be stored in the system and used as the expected position of the coil during PET reconstruction, thus making their location reproducible from scan to scan. In cases where flexible coils are used, or if the precision of the positioning of the rigid coil is insufficient, additional information about the localisation of the coil is required. This can be achieved by placing MR visible fiducial markers on the coil or by using an ultrashort or zero echo time MR imaging sequence [81]. In order to overcome the limitations of CT or TR derived AC maps with measurements on a different system, several upgraded methods have also been proposed, such as an in-situ transmission scan [86, 87], the use of computer-aided design files [88], or a maximumlikelihood reconstruction of attenuation and activity algorithm [89]. Although the attenuation of RF coils can be reduced substantially, there is currently no known strategy for building practically useable RF coils where the attenuation of the annihilation gammas can be completely neglected. Thus, it is important to consider the above-mentioned strategies when designing the RF coil and to use as few materials as possible. Currently, coil cases are mainly produced using 3D printed plastics, and the investigation of novel materials to this end could be useful. The selected materials, however, must fulfil the requirements of MR compatibility, mechanical and electrical safety regulations, and the PET requirements. As an example, a screen-printed coil technique has been recently introduced and can be used to print a predetermined or calculated coil array together with the coil holder [90]. By carefully selecting the materials, the desired stability and PET attenuation requirements can be achieved. Wirelessly operating metamaterial coils [91, 92] or lightweight coils [93] using new extremely-low-density materials could also be an ultimate option for simultaneous MR-PET and may eventually eliminate the necessity of attaining attenuation maps of the coil assembly.

Finally, these techniques are not only applicable to MRPET systems and may also be applied for other combined modalities, such as MR-X-ray [94], MR-SPECT [95, 96], and MR-Linear accelerator [97-99], which have similar constraints and requirements.

ACKNOWLEDGEMENT

C.-H.C, C.L. and N.J.S are funded in part by the Helmholtz Validation Fund, “Next generation BrainPET scanner for 7T MRI” Grant Nr. HVF-0051. The open access publication of this work was also funded by the Deutsche Forschungsgemeinschaft (DFG, German Research Foundation) – 491111487. The authors thank Ms Rick for English proofreading.

REFERENCES

[1] N. Weiskopf, L. J. Edwards, G. Helms, S. Mohammadi, and E. Kirilina,

“Quantitative magnetic resonance imaging of brain anatomy and in vivo

histology," Nat. Rev. Phys., vol. 3, pp. 570–588, 2021.

[2] A. Del Guerra, et al., "TRIMAGE: A dedicated trimodality (PET/MR/EEG) imaging tool for schizophrenia," Eur. Psychiat., vol. 50, pp. 7–20, 2018.

[3] N.J. Shah, "Multimodal neuroimaging in humans at 9.4 T: a technological breakthrough towards an advanced metabolic imaging scanner," Brain Struct. Funct., vol. 220, pp. 1867-1884, 2015.

[4] N.J. Shah, Hybrid MR-PET Imaging. Cambridge, UK, RSC, 2018.

[5] Neuner, et al., "Multimodal imaging utilising integrated MR-PET for human brain tumour assessment," Eur. Rad., vol. 22, pp. 2568-2580, 2012.

[6] N.J. Shah, et al., "Advances in multimodal neuroimaging: hybrid MRPET and MR-PET-EEG at 3 T and 9.4 T," J. Magn. Reson., vol. 229, pp. 101-115, 2013.

[7] M.S. Judenhofer, et al., "Simultaneous PET-MRI: a new approach for functional and morphological imaging," Nat. Med., vol. 14, pp. 459–465, 2008.

[8] H. Herzog, U. Pietrzyk, N.J. Shah, K. Ziemons, "The current state, challenges and perspectives of MR-PET," Neuroimage, vol. 49, pp. 2077-2082, 2010.

[9] S. Song, et al., "Simultaneous FET-PET and contrast-enhanced MRI based on hybrid PET/MR improves delineation of tumor spatial

biodistribution in gliomas: a biopsy validation study," Eur. J. Nucl. Med. Mol. Imaging vol. 47, pp. 1458–1467, 2020.

[10] B.J. Pichler, M.S. Judenhofer, H.F. Wehrl, "PET/MRI hybrid imaging: devices and initial results," Eur. Radiol., vol. 18, pp. 1077–1086, 2008.

[11] S. Yamamoto, H. Watabe, Y. Kanai, T. Watabe, M. Aoki, E. Sugiyama, K. Kato, J. Hatazawa, "Development of a flexible optical fiber based high resolution integrated PET/MRI system," Med. Phys., vol. 39, pp. 6660-71, 2012.

[12] T. Beyer and E. Moser, "MR/PET or PET/MRI: does it matter?," Magn. Reson. Mat. Phys. Biol. Med., vol. 26, pp. 1-4, 2013.

[13] C. Lerche, J. Felder, C.-H. Choi, and N.J. Shah, Hybrid MR-PET Imaging. Chapter 10, Cambridge, UK, RSC, 2018.

[14] M. Poole, R. Bowtell, D. Green, S. Pittard, A. Lucas, R. Hawkes, A. Carpenter, "Split gradient coils for simultaneous PET-MRI," Magn. Reson. Med., vol. 62, pp. 1106-1111, 2009.

[15] M. Oehmigen, M.E. Lindemann, L. Tellmann, T. Lanz, H.H. Quick, "Improving the CT (140 kVp) to PET (511 keV) conversion in PET/MR hardware component attenuation correction," Med. Phys. vol. 47, pp. 2116-2127, 2020.

[16] L. Tellmann, H.H. Quick, A. Bockisch, H. Herzog, T. Beyer, "The effect of MR surface coils on PET quantification in whole-body PET/MR: results from a pseudo-PET/MR phantom study," Med. Phys. vol. 38, pp.

2795-2805, 2011.

[17] Weirich, D. Brenner, J. Scheins, E. Besancon, L. Tellmann, H. Herzog, N.J. Shah, “Analysis and correction of count rate reduction during simultaneous MR-PET measurements with the BrainPET scanner,” IEEE Trans. Med. Imaging vol. 31, pp. 1372-1380, 2012.

[18] S.H. Keller, et al., “Image artifacts from MR-based attenuation correction in clinical, whole-body PET/MRI,” MAGMA. vol. 26, pp. 173-181, 2013.

[19] M. Eldib, et al., “Attenuation Correction for Magnetic Resonance Coils in Combined PET/MR Imaging: A Review,” PET Clinics, vol. 11, pp. 151–160, 2016.

[20] C.W. Lerche, et al., “PET attenuation correction for rigid MR Tx/Rx coils from 176Lu background activity,” Phys. Med. Biol., vol. 63, pp. 035039, 2018.

[21] J.E. Mackewn, et al., “Practical issues and limitations of brain attenuation correction on a simultaneous PET-MR scanner,” EJNMMI Physics, vol. 7, pp. 24, 2020.

[22] K. J. Hong, et al., “A prototype MR insertable brain PET using tileable GAPD arrays,” Med. Phys., vol. 40, pp. 042503-1, 2013.

[23] C.-H. Choi, et al., “Design, evaluation and comparison of endorectal coils for hybrid MR-PET imaging of the prostate,” Phys. Med. Biol., vol. 65, no. 11, p. 115005, 2020

[24] B.J. Lee, A.M. Grant, C.-M. Chang, R.D. Watkins, G.H. Glover, and

C.S. Levin, “MR Performance in the Presence of a Radio Frequency-Penetrable Positron Emission Tomography (PET) Insert for Simultaneous PET/MRI,” IEEE Trans. Med. Imaging, vol. 37, no. 9, pp. 2060–2069, 2018.

[25] P.D. Herrick, R.E. Ansorge, R.C. Hawkes, S.J. Sawiak, J.W. Stevick, T.A. Carpenter, “Radiofrequency coil design for simultaneous PET/MR systems,” IEEE Nucl. Sci. Symp. Med. Imaging Conf. pp. 2560-2567, 2010.

[26] A.A. Celik, C.-H. Choi, L. Tellmann, C. Rick, N. J. Shah, and J. Felder, “Design and Construction of a PET-Compatible Double-Tuned 1H/31P MR Head Coil,” IEEE Trans. Med. Imaging, vol. 40, no. 8, pp. 2015–2022, 2021.

[27] K. Lakshmanan, S. Dehkharghani, G. Madelin, and R. Brown, “A dualtuned 17O/1H head array for direct brain oximetry at 3 Tesla,” Magn. Reson. Med., vol. 83, no. 4, pp. 1512–1518, 2020.

[28] M. Oehmigen, et al., “A dual-tuned 13C/1H head coil for PET/MR hybrid neuroimaging: Development, attenuation correction, and first evaluation,” Med. Phys., vol. 45, no. 11, pp. 4877–4887, 2018.

[29] E.C. Hayes, W.A. Edelstein. J.F. Schenck, O.M. Mueller, and M. Eash, “An efficient highly homogeneous radiofrequency coil for wholebody NMR imaging at 1.5 T,” J. Magn. Reson., vol. 63, pp. 622-628, 1985.

[30] E. A. Barberi, J. S. Gati, B. K. Rutt, and R. S. Menon, “A transmitonly/ receive-only (TORO) RF system for high-field MRI/MRS applications,” Magn. Reson. Med., vol. 43, no. 2, pp. 284–289, 2000.

[31] P.B. Roemer, W.A. Edelstein, C.E. Hayes, S.P. Souza, and O.M. Mueller, “The NMR phased array,” Magn. Reson. Med., vol. 16, pp. 192-225, 1990.

[32] G. Wiggins, C. Triantafyllou, A. Potthast, A. Reykowski, M. Nittka, and L. l. Wald, “32-channel 3 Tesla receive-only phased-array head coil with soccer-ball element geometry,” Magn. Reson. Med., vol. 56, no. 1, pp. 216–223, 2006.

[33] M.A. Griswold, et al., “Generalized autocalibrating partially parallel acquisitions (GRAPPA),” Magn. Reson. Med., vol. 47, no. 6, pp. 1202–1210, 2002.

[34] D.A. Feinberg and K. Setsompop, “Ultra-fast MRI of the human brain with simultaneous multi-slice imaging,” J. Magn. Reson., vol. 229, pp. 90–100, 2013.

[35] Oh, et al., “An optimal RF shielding method for MR-PET fusion system with insertable PET,” International Journal of Imaging Systems and Technology, vol. 24, no. 3, pp. 263–269, 2014.

[36] C. Parl, et al., “A novel optically transparent RF shielding for fully integrated PET/MRI systems,” Phys. Med. Biol., vol. 62, no. 18, pp. 7357–7378, 2017.

[37] B.J. Peng, Y.Wu, S.R. Cherry, and J.H. Walton, “New shielding configurations for a simultaneous PET/MRI scanner at 7T,” J. Magn. Reson., vol. 239, pp. 50–56, 2014.

[38] B. Zhang, et al., “Effect of radiofrequency shield diameter on signal-tonoise ratio at ultra-high field MRI,” Magn. Reson. Med., vol. 85, no. 6, pp. 3522–3530, 2021.

[39] B.J. Lee, C.-M. Chang, C.S. Levin, PET System Technology Designs for Achieving Simultaneous PET/MRI. In: A. Iagaru, T. Hope, P. Veit-Haibach (eds) PET/MRI in Oncology. Cham, Switzerland, Springer, 2018.

[40] B.J. Lee, R.D. Watkins, K.S. Lee, C.-M. Chang, and C.S. Levin, “Performance evaluation of RF coils integrated with an RF-penetrable PET insert for simultaneous PET/MRI,” Magn. Reson. Med., vol. 81, no. 2, pp. 1434–1446, 2019.

[41] A.M. Grant, B.J. Lee, C.-M. Chang, and C.S. Levin, “Simultaneous PET/MR imaging with a radio frequency-penetrable PET insert,” Med. Phys., vol. 44, no. 1, pp. 112–120, 2017.

[42] C.-M. Chang, B.J. Lee, A.M. Grant, A.N. Groll, and C.S. Levin, “Performance Study of a Radio-Frequency Field-Penetrable PET Insert for Simultaneous PET/MRI,” IEEE Transactions on Radiation and Plasma Medical Sciences, vol. 2, no. 5, pp. 422–431, 2018.

[43] M.S.H. Akram, T. Obata, M. Suga, F. Nishikido, E. Yoshida, K. Saito,

T. Yamaya, “MRI compatibility study of an integrated PET/RF-coil prototype system at 3T,” J. Magn. Reson., vol. 283, pp. 62-70, 2017.

[44] M.S.H. Akram, T. Obata, T. Yaaya, “Microstrip transmission line RF coil for a PET/MRI insert,” Magn. Reson. Med. Sci. vol. 19, pp.147-153, 2020.

[45] X. Yan, J.C. Gore, and W.A. Grissom, “A mixed dipole and microstrip transmit/receive array,” Proc Intl Soc Magn Reson Med, vol. 24, pp. 2140, 2016.

[46] C.-H. Choi, S.-M. Hong, J. Felder, C. Lerche and N.J. Shah, “Simulation of a shield effect on a J-pole antenna array for ultra-high field MRPET,” Proc Intl Soc Magn Reson Med, vol. 31, pp.3948, 2022.

[47] M.S.H. Akram, C.S. Levin, T. Obata, G. Hirumi, and T. Yamaya, “Geometry optimization of electrically floating PET inserts for improved RF penetration for a 3 T MRI system,” Med. Phys., vol. 45, no. 10, pp. 4627–4641, 2018.

[48] Etxebeste, et al., “Study of sensitivity and resolution for full ring PET prototypes based on continuous crystals and analytical modelling of the light distribution,” Phys. Med. Biol., vol. 64, pp. 035015, 2019.

[49] M.E. Ladd, et al., “Pros and cons of ultra-high-field MRI/MRS for human application,” Prog. Nucl. Magn. Reson. Spectrosc. vol. 109, pp. 1–50, 2018.

[50] I. Neuner, T. Veselinović, S. Ramkiran, R. Rajkumar, G.J.

Schnellbaecher, and N.J. Shah, “7T ultra-high-field neuroimaging for mental health: an emerging tool for precision psychiatry?,” Transl. Psychiatry, vol. 12, no. 1, pp. 1–10, 2022.

[51] T. Platt, M.E. Ladd, and D. Paech, “7 Tesla and Beyond: Advanced Methods and Clinical Applications in Magnetic Resonance Imaging,” Investigative Radiology, vol. 56, no. 11, pp. 705–725, 2021.

[52] O. Kraff, A. Fischer, A.M. Nagel, C. Mönninghoff, and M.E. Ladd, “MRI at 7 tesla and above: Demonstrated and potential capabilities,” J. Magn. Reson. Imaging, vol. 41, pp. 13–33, 2015.

[53] C.W. Lerche, et al., “Design and estimated performance of a UHF-MRI compatible BrainPET insert for neuroscience,” IEEE NSS/MIC, pp. 1130, 2020.

[54] I. Schug. et al., “Initial PET performance evaluation of a preclinical insert for PET/MRI with digital SiPM technology,” Phys. Med. Biol., vol. 61, no. 7, pp. 2851–2878, 2016.

[55] J.Y. Won. et al., ‘Development and Initial Results of a Brain PET Insert for Simultaneous 7-Tesla PET/MRI Using an FPGA-Only Signal Digitization Method,” IEEE Trans. Med. Imaging, vol. 40, no. 6, pp. 1579–1590, 2021.

[56] A.J.E. Raaijmakers, et al., “The fractionated dipole antenna: A new antenna for body imaging at 7 Tesla,” Magn. Reson. Med. vol. 75, pp. 1366–1374, 2016.

[57] C.-H. Choi, et al., “A novel J-shape antenna array for simultaneous MRPET or MR-SPECT imaging,” IEEE Trans. Med. Imaging, vol. 41, pp. 1104-1113, 2022.

[58] I.R.O. Connell and R.S. Menon, “Shape Optimization of an Electric Dipole Array for 7 Tesla Neuroimaging,” IEEE Trans. Med. Imaging, vol. 38, no. 9, pp. 2177–2187, 2019.

[59] S.-M. Hong, J.H. Park, M.-K. Woo, Y.-B. Kim, and Z.-H. Cho, “New design concept of monopole antenna array for UHF 7T MRI,” Magn. Reson. Med., vol. 71, no. 5, pp. 1944–1952, 2014.

[60] D.O. Brunner, N. De Zanche, J. Fröhlich, J. Paska, K.P. Pruessmann, “Travelling-wave nuclear magnetic resonance,” Nat. vol. 457, pp. 994–998, 2009.

[61] I. Padormo, A. Beqiri, J.V. Hajnal, and S.J. Malik, “Parallel transmission for ultrahigh-field imaging,” NMR in Biomedicine, vol. 29, no. 9, pp. 1145–1161, 2016.

[62] S. Orzada, et al., “A 32-channel parallel transmit system add-on for 7T MRI,” PLoS ONE, vol. 14, no. 9, pp. e0222452, 2019.

[63] M.A. Ertürk, A.J. Raaijmakers, G. Adriany, K. Uğurbil, and G.J. Metzger, “A 16-channel combined loop-dipole transceiver array for 7 Tesla body MRI,” Magn. Reson. Med., vol. 77, no. 2, pp. 884-894, 2017.

[64] B. Steensma, et al., “Introduction of the snake antenna array: Geometry optimization of a sinusoidal dipole antenna for 10.5T body imaging with

lower peak SAR," Magn. Reson. Med. vol. 84, pp. 2885–2896, 2020.

[65] A.S.M.Z. Kausar, D.C. Reutens, E. Weber, and V. Vegh, "Monopole antenna array design for 3 T and 7 T magnetic resonance imaging," PLoS ONE, vol. 14, no. 4, p. e0214637, 2019.

[66] M.K. Woo, et al., "Comparison of 16-Channel Asymmetric Sleeve Antenna and Dipole Antenna Transceiver Arrays at 10.5 Tesla MRI," IEEE Trans. Med. Imaging, vol. 40, no. 4, pp. 1147–1156, 2021.

[67] C.-H. Choi, et al., "Dipolantennen-Array für hybride MR-PET und MR SPECT Tomographen sowie dessen Verwendung und MR-PET oder MR-SPECT Tomograph mit einem Dipolantennen-Array," DE102019003949A1, 2020.

[68] C.-H. Choi, L. Tellmann, J. Felder, C. Lerche, and N.J. Shah, "An evaluation of RF coil materials for 1H/31P for use in a hybrid MR-PET scanner at 3T," Proc Intl Soc Magn Reson Med, vol. 25, pp. 4432, 2017.

[69] L. Tellmann, H. Herzog, F. Boers, C. Lerche, and N. J. Shah, "Alternative headphones for patient noise protection and communication in PET-MR studies of the brain," EJNMMI Res, vol. 8, no. 1, pp. 106, 2018.

[70] T. Heußer, C.M. Rank, Y. Berker, M. T. Freitag, and M. Kacherlrieß, "MLAA-based attenuation correction of flexible hardware components in hybrid PET/MR imaging," EJNMMI Phys., vol. 4, pp. 12, 2017.

[71] R. Manavaki, Y.T. Hong, and T.D. Fryer, "Brain MRI Coil Attenuation

Map Processing for the GE SIGNA PET/MR: Impact on PET Image Quantification and Uniformity," IEEE NSS/MIC, 2019.

[72] T. hope, K.V. Keu, F. Robb, R. Herfkens and A. Iagaru, "Effect of anterior body MRI coils on PET acquisitions and evaluation of a novel minimally attenuating PET/MR coil," J. Nucl. Med., vol. 54, pp. 2170, 2013.

[73] C.Y. Sander, et al., "A 31-channel MR brain array coil compatible with positron emission tomography," Magn. Reson. Med. vol. 73, pp. 2363–2375, 2015.

[74] U.C. Anazodo, et al., "Assessment of PET performance of a 32-Channel MR Brain Array Head Coil Compatible with PET for Integrated PETMRI," Proc. 7th conference on PET/MR and SPECT/MR, 2016.

[75] Y.-J. Stickle, M. Giancola, C.K. Follante, T. Stickle, F. Robb, H. Blahnik and T.-Y. Yang, "A novel PET optimized head neck coil for 3T simultaneous MRPET system," Proc Intl Soc Magn Reson Med, vol. 31, pp.1289, 2022.

[76] L. Yin, F. Schrank, N. Gross-Weege, D. Schug, and V. Schulz, "RF shielding materials for highly-integrated PET/MRI systems," Phys. Med. Biol., vol. 66, no. 9, pp. 09NT01, 2021.

[77] A. Destruel, J. Jin, E. Weber, M. Li, C. Engstrom, F. Liu, and S. Crozier, "Integrated multi-modal antenna with coupled radiating structures (IMARS) for 7T pTx body MRI," IEEE Trans. Med. Imaging, vol. 41, pp.

39-51, 2022.

[78] D. Truhn, F. Kiessling, and V. Schulz, “Optimized RF shielding techniques for simultaneous PET/MR,” Med. Phys., vol. 38, no. 7, pp. 3995–4000, 2011.

[79] N. Moghadam, R. Espagnet, J. Bouchard, R. Lecomte, and R. Fontaine, “Studying the effects of metallic components of PET-insert on PET and MRI performance due to gradient switching,” Phys. Med. Biol., vol. 64, no. 7, pp. 075003, 2019.

[80] B.J. Lee, R.D. Watkins, C.M. Chang, and C.S. Levin, “Low eddy current RF shielding enclosure designs for 3T MR applications,” Magn. Reson. Med., vol. 79, pp. 1745–1752, 2018.

[81] D.H. Paulus and H.H. Quick, “Hybrid positron emission tomography/magnetic resonance imaging: challenges, methods, and state of the art of hardware component attenuation correction,” Investigative radiology, vol. 51, pp. 624-634, 2016.

[82] A. Renner, et al., “A head coil system with an integrated orbiting transmission point source mechanism for attenuation correction in PET/MRI,” Phys. Med. Biol., vol. 63, pp. 225014, 2018.

[83] D.H. Paulus, L. Tellmann, and H.H. Quick, "Towards improved hardware component attenuation correction in PET/MR hybrid imagin," Phys. Med. Biol., vol. 58, pp. 8021-8040, 2013.

[84] J.P. Carney, D.W. Townsend, V. Rappoport, and B. Bendriem, “Method

for transforming CT images for attenuation correction in PET/CT imaging," Med. Phys., vol. 33, pp. 976-983, 2006.

[85] R.A. Stark, M. Cervo, J.A. Nye, and J.N. Aarsvold, "Estimation of MRcoil attenuation in the simultaneous PET/MR BrainPET," IEEE NSS/MIC, pp. 3563-3565, 2010.

[86] P. Mollet, V. Keereman, J. Bini, D. Izquierdo-Garcia, Z.A. Fayad, and S. Vandenberghe, "Improvement of attenuation correction in time-of-flight PET/MR imaging with a positron-emitting source," J. Nucl. Med., vol. 55, pp. 329-336, 2014.

[87] A. Farag, R.T. Thompson, J.D. Thiessen, F.S. Prato, and J. Théberge, "Improved PET/MRI accuracy by use of static transmission source in empirically derived hardware attenuation correction," EJNMMI physics, vol. 8, pp. 1-16, 2021.

[88] M.E. Lindemann, M. Oehmigen, T. Lanz, H. Grafe, N.M. Bruckmann, L. Umutlu, and H.H. Quick, "CAD-based hardware attenuation correction in PET/MRI: First methodical investigations and clinical application of a 16-channel RF breast coil," Med. Phys., vol. 48, pp. 6696-6709, 2021.

[89] T. Heußer, C.M. Rank, Y. Berker, M.T. Freitag, and M. Kachelrieß, "MLAA-based attenuation correction of flexible hardware components in hybrid PET/MR imaging," EJNMMI physics, vol. 4, pp. 1-23, 2017.

[90] J. R. Corea, et al., "Screen-printed flexible MRI receive coils," Nat.

Commun., vol. 7, no. 1, pp. 10839, 2016.

[91] A. Shchelokova, et al., “Ceramic resonators for targeted clinical magnetic resonance imaging of the breast,” Nat. Commun., vol. 11, no. 1, pp. 3840, 2020.

[92] E. Stoja, et al., “Improving magnetic resonance imaging with smart and thin metasurfaces,” Sci. Rep., vol. 11, no. 1, p. 16179, 2021.

[93] T.W. Deller, N.K. Mathew, S.A. Hurley, C.M. Bobb, and A.B. McMillan, “PET Image Quality Improvement for Simultaneous PET/MRI with a Lightweight MRI Surface Coil,” Radiology, vol. 298, no. 1, pp. 166–172, 2021.

[94] V. Rieke, et al., “X-ray compatible radiofrequency coil for magnetic resonance imaging,” Magn. Reson. Med., vol. 53, no. 6, pp. 1409–1414, 2005.

[95] B.F. Hutton, et al., “Development of clinical simultaneous SPECT/MRI,” Br. J. Radiol. vol. 91, pp. 20160690, 2017.

[96] M. Carminati, et al., “Validation and Performance Assessment of a Preclinical SiPM-Based SPECT/MRI Insert,” IEEE Transactions on Radiation and Plasma Medical Sciences, vol. 3, no. 4, pp. 483–490, 2019.

[97] S.E. Zijlema, W. Branderhorst, R. Bastiaannet, R.H.N. Tijssen, J.J.W. Lagendijk, and C.A.T. van den Berg, “Minimizing the need for coil attenuation correction in integrated PET/MRI at 1.5 T using low-density

MR-linac receive arrays," Phys. Med. Biol., vol. 66, no. 20, p. 20NT01, 2021.

[98] S.E. Zijlema, et al., "Design and feasibility of a flexible, on-body, high impedance coil receive array for a 1.5 T MR-linac," Phys. Med. Biol., vol. 64, no. 18, p. 185004, 2019.

[99] B.W. Raaymakers, et al., "Integrating a 1.5 T MRI scanner with a 6 MV accelerator: proof of concept," Phys. Med. Biol., vol. 54, no. 12, pp. N229–N237, 2009.